



This is a repository copy of *Metal recovery from jarosite waste - A resin screening study*.

White Rose Research Online URL for this paper:

<http://eprints.whiterose.ac.uk/122846/>

Version: Accepted Version

---

**Article:**

Riley, A.L., Pepper, S.E., Canner, A.J. et al. (2 more authors) (2018) Metal recovery from jarosite waste - A resin screening study. *Separation Science and Technology*, 53 (1). pp. 22-35. ISSN 0149-6395

<https://doi.org/10.1080/01496395.2017.1378679>

---

This is an Accepted Manuscript of an article published by Taylor & Francis in *Separation Science and Technology* on 25/09/2017, available online:

<http://www.tandfonline.com/10.1080/01496395.2017.1378679>

**Reuse**

Items deposited in White Rose Research Online are protected by copyright, with all rights reserved unless indicated otherwise. They may be downloaded and/or printed for private study, or other acts as permitted by national copyright laws. The publisher or other rights holders may allow further reproduction and re-use of the full text version. This is indicated by the licence information on the White Rose Research Online record for the item.

**Takedown**

If you consider content in White Rose Research Online to be in breach of UK law, please notify us by emailing [eprints@whiterose.ac.uk](mailto:eprints@whiterose.ac.uk) including the URL of the record and the reason for the withdrawal request.



[eprints@whiterose.ac.uk](mailto:eprints@whiterose.ac.uk)  
<https://eprints.whiterose.ac.uk/>

## 1 **Metal recovery from jarosite waste - A resin screening study**

2

3 Alex L. Riley\* , Sarah E. Pepper, Adam J. Canner, Solomon F. Brown, Mark D. Ogden

4

5 Separations and Nuclear Chemical Engineering Research (SNUCER) Group, Department of

6 Chemical and Biological Engineering, University of Sheffield, Sheffield, S1 3JD, United

7 Kingdom.

8

9 \*Corresponding author's email: [ariley4@sheffield.ac.uk](mailto:ariley4@sheffield.ac.uk)

10

11 **Abstract** — Work has been carried out screening hydrometallurgical resins for application in  
12 the valorization of industrially produced jarosite. Of the seven resins tested, anion exchange  
13 resins performed poorly for valuable metal recovery. Purolite S950+ and S957, along with a  
14 strong acid resin, show good extraction properties but are selective for Fe<sup>3+</sup> over the other  
15 (divalent) metals. Purolite S930+ (iminodiacetic acid-functionalized resin) demonstrates  
16 selectivity for Cu<sup>2+</sup> over Fe<sup>3+</sup> but poor selectivity for Ni<sup>2+</sup>, Zn<sup>2+</sup> and Co<sup>2+</sup>. Dowex M4195  
17 (bispicolylamine-functionalized resin) demonstrates promise for extracting metals of value  
18 away from a mixed metal pregnant liquor solution (PLS). A three-stage column based  
19 recovery process is proposed for jarosite leachate treatment.

20

21

22

23

24

25 **Keywords**— ion exchange, resource recovery, extraction, transition metals, acid mine  
26 drainage

## 27 **1 INTRODUCTION**

28 Industrially produced jarosite can pose significant environmental threats due to the toxic metal  
29 impurities present in its structure; typically of the form  $AM_3(OH)_6(SO_4)_2$ , where  $M = Fe^{3+}$ .  
30 Commonly produced as a by-product of the hydrometallurgical refinement of zinc from  
31 sulphide ores, the impurities present in the waste include Cu, Pb, Zn, Mn, Cd, Al, Cr, Ni, and  
32 Co. Major quantities of jarosite are generated in China, USA, Canada, Japan, Australia, and  
33 across Europe [1], with India producing approximately 142,000 Tonnes per annum of jarosite  
34 type slag as solid waste from the lead and zinc smelting industries [2]. The current method of  
35 disposal for industrial jarosite is in open tailing dumps, where the waste is subject to  
36 atmospheric weathering, leading to the mobilization of dissolved metals in acidic leachates  
37 [3]. The environmental impact following the release of such leachates from jarosite waste  
38 depositories is comparable to that of acid mine drainage, whereby downstream ecological  
39 populations are adversely affected through elevated metal concentrations and reduced pH  
40 [4,5]. For this reason, the reduction in concentration of problematic metals within jarosite  
41 wastes is a desired step before disposal and/or material reuse. Despite causing  
42 environmental damage, some of the metal impurities present within the waste have an  
43 intrinsic value which may provide an opportunity for recovery [6]. An approximate composition  
44 of an industrial jarosite is given in Table 1 [1-3, 6-8], with prices per tonne for each metal  
45 taken from the London Metals Exchange (November 2016) [8]. In the most optimistic  
46 circumstances the jarosite waste generated per annum could return a resource recovery  
47 value of between £28-49 million. There is little associated value to recovering the Fe, and the  
48 Cd and Pb content has not been included in this assessment.

49  
50 This research is an initial study focusing on the application of ion exchange resins for the  
51 recovery of metals with inherent value from jarosite wastes. The study is based on the  
52 premise that the jarosite would be crushed, roasted with sulfuric acid, and leached with water

53 to produce a metal-rich PLS prior to treatment. Ion exchange resins, particularly exchangers  
54 with the capacity for chelate formation, are able to remove specific metal ions from solution  
55 present in low concentrations [9]. A wide range of ion exchange resins are available  
56 commercially, with different functional groups targeted towards different applications. The  
57 resins to be screened in this work contain a variety of functional groups, namely; polyamine,  
58 bispicolylamine, amidoxime, aminophosphonic, iminodiacetic acid, phosphonic acid, and  
59 sulfonic acid groups supported by a macroporous polymer backbone (generally polystyrene-  
60 DVB). Functionalized ion exchange resins have seen application in a wide range of industrial  
61 processes, including the removal of platinum group metals (PGMs) from spent catalyst  
62 solutions [10], the removal of vanadium from alkaline wastes [11, 12], and sorption of Ni and  
63 Cu from low-grade ores [13].

64

65 The aim of this initial screening process is to identify the resin functionalities most suitable for  
66 the specific removal of metals from sulfuric acid and sulfate media, as would be expected  
67 following a sulfuric leaching process. This is the first comprehensive hydrometallurgical resin  
68 screening study for jarosite treatment, and the results will help to shape an eventual multi-  
69 column ion exchange based resource recovery process. Through the development of an  
70 effective process for metal recovery, a commercial value is ascribed to what would otherwise  
71 be treated as a waste product, diverting material away from disposal and reducing the  
72 potential for environmental damage.

73

## 74 **2 EXPERIMENTAL**

75

### 76 **2.1 Reagents and stock solutions**

77 All chemicals used were of analytical grade and purchased from Sigma–Aldrich unless  
78 otherwise specified. For experimental investigations the ion exchangers Dowex M4195 and

79 Dowex M31 were supplied by Sigma-Aldrich, and the rest of the resins screened were  
80 donated by Purolite. An overview of the characteristics of resins screened in this work are  
81 provided in Table 2 and Figure 1. Prior to experimentation, resins were preconditioned by  
82 bottle rolling with 1 M H<sub>2</sub>SO<sub>4</sub> for 24 hrs at room temperature. Resins were washed five times  
83 with 200 bed volumes (BV) of deionized water before use to remove any residuals left over  
84 from the preconditioning process.

85 A mixed metal (2000 ppm each) stock solution of Al(III), Co(II), Cu(II), Fe(III), Ni(II), Mn(II) and  
86 Zn(II) was prepared by dissolving their respective sulfate salts in sulfuric acid at pH 1.0.

87 Aliquots of this were taken to make a synthetic pregnant liquor solution (PLS). Metal analysis  
88 was carried out using either a Perkin Elmer Atomic Absorption Spectrometer AAnalyst 400 or  
89 a Thermo Scientific iCAP 6000 series ICP-OES. Calibration for both instruments was  
90 performed using standard solutions diluted with 1% nitric acid as required.

91

## 92 **2.2 Metal loading experiments as a function of pH and sulfate concentration**

93 A fixed volume of wet settled resin was contacted with a fixed volume of solution containing  
94 metals at a set pH and shaken on a mechanical shaker for 24 hours. The pH was controlled  
95 using dilute solutions of sulfuric acid. Upon reaching equilibrium, the resin was left to settle  
96 under gravity before the solution pH was measured and an aliquot taken for elemental  
97 analysis. Uptake was determined by concentration difference between the initial solution and  
98 the solution post-contact. The extraction percentage (E%) was calculated as follows:

$$99 \quad E\% = (C_i - C_e)/C_i \times 100 \quad (1)$$

100 Where C<sub>i</sub> is the initial concentration of metal and C<sub>e</sub> is the concentration of metal in solution at  
101 equilibrium. pH measurements for solutions were determined using a silver/silver chloride  
102 reference electrode calibrated from pH 1-10 using standard buffer solutions. At higher acid  
103 concentrations, [H<sup>+</sup>] were determined by titration. Error margins were calculated through  
104 triplicate sampling and analysis of aqueous solutions prior to contact with exchange resins.

## 105 **3 RESULTS**

106

### 107 **3.1 Weak base and strong base functionalised resins**

108 It was observed that the weak base polyamine-functionalized resin S985 was not effective  
109 for metal removal from sulfuric acid media regardless of  $[H^+]$ , with extraction rarely  
110 exceeding 20% (Figure 2). Conversely, the bispicolylamine-functionalized resin M4195  
111 displayed effective performance for several elements, particularly  $Cu^{2+}$ , which was  
112 quantitatively extracted until  $[H^+]$  exceeded 1 M (Figure 3). A distinct relationship between  
113 solution pH and removal of  $Ni^{2+}$  by M4195 was revealed, with a vast difference in uptake  
114 efficiency over the studied conditions. The reduction in extraction with increased  $[H^+]$  was  
115 also exhibited for  $Co^{2+}$ ,  $Zn^{2+}$ , and  $Fe^{3+}$ , though not to the same extent as for  $Ni^{2+}$ . Removal of  
116  $Al^{3+}$  and  $Mn^{2+}$  was minimal under all conditions of pH, indicating poor selectivity towards  
117 these metals by M4195. As such, the selectivity series for M4195 may be defined as  $Cu^{2+} \gg$   
118  $Fe^{3+} > Ni^{2+} > Co^{2+} = Zn^{2+} = Mn^{2+} = Al^{3+}$  at low pH, with selectivity at higher pH switching to  
119  $Cu^{2+} = Ni^{2+} > Zn^{2+} > Co^{2+} > Fe^{3+} > Mn^{2+} = Al^{3+}$ . The  $pH_{50}$  values, representing the pH at which  
120 50% extraction is obtained, for each metal species is given in Table 3 for M4195. For  $Cu^{2+}$ ,  
121 where extraction exceeded 50% over the complete pH range studied, a 4-point linear  
122 regression method was used to determine the  $pH_{50}$  values. The percentage extraction by  
123 M4195 on selected metal ions as a function of increasing ammonium sulfate concentration at  
124 pH 1.55 is shown in Figure 4. The addition of sulfate to the PLS did not affect the strong  
125 selectivity of M4195 towards  $Cu^{2+}$  and  $Ni^{2+}$ , with continued quantitative extraction of these  
126 metals. For  $Co^{2+}$ ,  $Zn^{2+}$ , and  $Fe^{3+}$ , increases in solution sulfate concentration were  
127 accompanied by modest increases in their extraction, with improvements of approximately  
128 8%, 10%, and 16%, respectively (Figure 4). Extraction of  $Al^{3+}$  and  $Mn^{2+}$  remained poor, with  
129 little response to sulfate addition. The selectivity series for M4195 at pH 1.55 was not  
130 affected by sulfate addition and remained constant as  $Cu^{2+} = Ni^{2+} > Co^{2+} > Zn^{2+} > Fe^{3+} >$

131  $Mn^{2+} = Al^{3+}$ . Sulfate screening experiments were not performed for S985 given its poor  
132 selectivity towards the elements studied (Figure 2).

133

134 The effect of sulfuric acid concentration on the extraction of metals from simulant jarosite  
135 leach solution by the amidoxime functionalised resin S910 is provided in Figure 5. It was  
136 observed that the resin was most selective for  $Fe^{3+}$ , with poor extraction of other metals over  
137 the studied range. An increase in Fe extraction was observed between 0.05 and 0.5 M  $H^+$   
138 indicative of a change in extraction mechanism at this point, but this had little effect on the  
139 extraction of the other metals in solution. At lower  $[H^+]$ ,  $Cu^{2+}$  extraction did increase to  
140 approximately 28%, but  $Fe^{3+}$  was still preferentially extracted (Figure 5). Given that S910  
141 showed poor selectivity towards the elements of intrinsic value in the simulant solution, it  
142 was not considered suitable for purpose within the jarosite treatment system, and no further  
143 experimental work was performed for this resin.

144

### 145 **3.2 Weak acid functionalised resins**

146 The extraction of metals from jarosite leach simulant by the weak acid resin S950+,  
147 containing aminophosphonic acid functionality, is shown in Figure 6. A preference towards  
148 the extraction of trivalent  $Fe^{3+}$  and  $Al^{3+}$  over the divalent transition elements is exhibited by  
149 S950+, with complete extraction for  $Fe^{3+}$  irrespective of  $[H^+]$ , and extraction of  $Al^{3+}$  only  
150 diminishing by 20% under high acid concentration (Figure 6). The extraction of other  
151 elements in solution was suppressed gradually as  $[H^+]$  increased, with almost exclusive  
152 extraction of  $Fe^{3+}$  and  $Al^{3+}$  by 4 M  $H^+$ . The selectivity series for S950+ can be described at  
153 lower  $[H^+]$  as  $Fe^{3+} > Al^{3+} > Mn^{2+} > Cu^{2+} > Zn^{2+} > Co^{2+} > Ni^{2+}$ , switching to  $Fe^{3+} > Al^{3+} \gg Mn^{2+}$   
154  $> Zn^{2+} > Co^{2+} = Ni^{2+} = Cu^{2+}$  at higher  $[H^+]$ .

155 The addition of ammonium sulfate to solutions in contact with S950+ at pH 1.40 had no  
156 effect on its  $Fe^{3+}$  extraction efficiency (Figure 7). As ammonium sulfate concentration

157 increases to 2 M, the extraction of all other metal ions is suppressed before increasing again  
158 above 2 M sulfate for  $\text{Mn}^{2+}$ ,  $\text{Cu}^{2+}$ , and  $\text{Zn}^{2+}$  (Figure 7), potentially suggesting an alternative  
159 extraction mechanism under these conditions. The extraction of  $\text{Co}^{2+}$  and  $\text{Ni}^{2+}$  does not  
160 increase above 2 M sulfate, and remains unaffected by the resin functionality (Figure 7).

161

162 The results of pH screening for the iminodiacetic acid-functionalized resin S930+ is  
163 presented in Figure 8. At lower  $\text{H}^+$  concentrations, S930+ shows high selectivity towards  
164  $\text{Cu}^{2+}$  and  $\text{Fe}^{3+}$ , with reasonable removal of  $\text{Ni}^{2+}$  also. The addition of sulfuric acid to the  
165 simulant solution has a drastic adverse effect on the metal removal capabilities of this resin,  
166 with extraction under 8% for all studied metals beyond 1 M  $\text{H}^+$  (Figure 8). As such, this resin  
167 would be more suitable for operation at higher pH, where the selectivity series can be  
168 described as  $\text{Cu}^{2+} > \text{Fe}^{3+} > \text{Ni}^{2+} > \text{Co}^{2+} > \text{Zn}^{2+} > \text{Al}^{3+} = \text{Mn}^{2+}$ .

169 The effect of ammonium sulfate addition on the uptake efficiencies of S930+ towards each  
170 metal was studied at pH 1.45 (Figure 9). Increasing the concentration of sulfate in solution  
171 results in a steady improvement in the extraction of  $\text{Ni}^{2+}$ ,  $\text{Co}^{2+}$ , and  $\text{Zn}^{2+}$ , with little effect on  
172 removal of  $\text{Al}^{3+}$  and  $\text{Mn}^{3+}$ . Quantitative extraction was observed for  $\text{Cu}^{2+}$  under all sulfate  
173 concentrations, with only minor suppression of  $\text{Fe}^{3+}$  extraction after 3 M sulfate (Figure 9).

174 The  $\text{pH}_{50}$  values for S950+ and S930+ are given in Table 4.

175

### 176 **3.3 Strong acid functionalised resins**

177 The static extraction of metals from the PLS by strong acid resin S957 containing mixed  
178 phosphonic acid and sulfonic acid functionality is shown in Figure 10. The S957 resin is  
179 selective for  $\text{Fe}^{3+}$  over all the other metals in the PLS and also appears to be a good  
180 extractant for  $\text{Al}^{3+}$ . With increased addition of sulfuric acid, a sharp reduction in extraction  
181 capability is observed for most metals, with the exception of  $\text{Fe}^{3+}$ . The surface functionality of  
182 S957 shows very little separation capability for first row transition metals (Figure 10). The

183 resulting selectivity series for S957 at low pH follows the order of  $\text{Fe}^{3+} > \text{Al}^{3+} > \text{Mn}^{2+} = \text{Cu}^{2+} =$   
184  $\text{Zn}^{2+} = \text{Co}^{2+} = \text{Ni}^{2+}$ .

185

186 The effects of ammonium sulfate addition at pH 1.35 on the extraction of metals by S957, is  
187 presented in Figure 11. The increased sulfate concentration appears to have little effect on  
188 the extraction of  $\text{Fe}^{3+}$  and  $\text{Al}^{3+}$  by the resin, with only a minor drop in extraction for  $\text{Al}^{3+}$   
189 beyond 1 M sulfate. For the other elements studied, a detrimental decrease in extraction  
190 efficiency is observed, leading ultimately to metal extraction under 20% beyond 1 M sulfate.

191

192 The final resin tested as part of this initial screening study was the sulfonic acid  
193 functionalised resin M31. This resin appeared to be highly effective at removing all metal  
194 species present in the jarosite leach simulant, with very high extraction percentages at low  
195  $[\text{H}^+]$  (Figure 12). However, as the concentration of sulfuric acid in the simulant was  
196 increased, a very sharp decline in its capacity for removal was observed; dropping to under  
197 20% for all metal species beyond 1 M  $\text{H}^+$ . A similar pattern was observed for its extraction  
198 potential as a factor of ammonium sulfate addition at pH 1.45 (Figure 13), with decreased  
199 extraction at higher sulfate concentrations. The  $\text{pH}_{50}$  values for the extraction of each metal  
200 species by S957 and M31 are provided in Table 5, as calculated from metal extraction  
201 curves.

202

## 203 **4 DISCUSSION**

204

### 205 **4.1 Weak base and strong base functionalised resins**

206 It is clear from the results collected that for the anion exchange resins tested, particularly  
207 S985, to be effective for the targeted metal extraction of first row transition metals from  
208 sulfuric acid media; either higher pH values are required, or extraction needs to be performed

209 in a more non-polar medium such as mixed aqueous methanol or dimethyl sulfoxide [14].  
210 Dowex M4195 is a weak base chelating resin with bispicolylamine functionality which shows  
211 unique separation capabilities for first row transition metals from sulfuric acid (Figure 3). The  
212 selectivity of M4195 for  $\text{Cu}^{2+}$  over  $\text{Fe}^{3+}$  has been previously noted in the literature [15], which  
213 presented loading capacities from 120 g/L  $\text{H}_2\text{SO}_4$ , however the effect of  $[\text{H}^+]$  on the degree of  
214 extraction was not shown. The pH dependent removal of  $\text{Co}^{2+}$ ,  $\text{Ni}^{2+}$ ,  $\text{Zn}^{2+}$  and  $\text{Mn}^{2+}$  have been  
215 detailed previously for M4195 from HCl solutions [16]. Changing from HCl to  $\text{H}_2\text{SO}_4$  media  
216 does little to change the extraction trend [17]. From the data presented (Figure 2 and 3)  
217 M4195 seems to be the best choice for targeting  $\text{Co}^{2+}$ ,  $\text{Ni}^{2+}$ ,  $\text{Cu}^{2+}$  and  $\text{Zn}^{2+}$ , and some  $\text{Fe}^{3+}$ ,  
218 away from  $\text{Mn}^{2+}$  and  $\text{Al}^{3+}$  in the simulated jarosite leach solution. The increase in ammonium  
219 sulfate in solution has a slightly positive effect on the uptake of metals by M4195, indicating  
220 that the most probable interaction mechanism is by chelation with first row transition metals  
221 [18] apart from  $\text{Fe}^{3+}$ . Taking into account speciation [19] the interaction of ferric ion with  
222 M4195 is most likely through an ion exchange mechanism.

223 To determine the effectiveness of M4195 for metal recovery from a jarosite PLS more  
224 experiments are required regarding loading capacities and dynamic processing data.  
225 The extraction of metal ions by S910 from sulfuric acid (Figure 5) indicated poor performance  
226 for targeted metal recovery from the solutions tested. At strongly acidic pH, S910 resin is  
227 more selective for  $\text{Fe}^{3+}$  than the other metal species present. The noted change in extraction  
228 behavior of  $\text{Fe}^{3+}$  is most likely attributed to the hydrolysis of the anionic ferric sulfate species  
229 in solution [19]. Previously this resin had been tested for  $\text{Zn}^{2+}$ ,  $\text{Ni}^{2+}$ , and  $\text{Cu}^{2+}$  uptake from HCl  
230 media [20] and showed better performance in the pH region of 2-4 for  $\text{Cu}^{2+}$  uptake with  $\text{Ni}^{2+}$   
231 and  $\text{Zn}^{2+}$  extraction starting at pH 3.5. This marginal selectivity for  $\text{Cu}^{2+}$  does not seem to  
232 change when comparing  $\text{H}_2\text{SO}_4$  media with HCl [20]. From the data presented it is clear  
233 under the acidic sulfate conditions tested that the metals cannot effectively compete with

234 proton for the amidoxime functionality, resulting in the suppression of S910 extraction at high  
235  $[H^+]$  (Figure 5).

236

#### 237 **4.2 Weak acid functionalised resins**

238 In testing the extractive capabilities of aminophosphonic and iminodiacetic acid functionalized  
239 resins, the role of  $[H^+]$  as a limiting factor for metal extraction became apparent (Figure 6 and  
240 8, respectively). The low extraction of metals by S950+ and S930+ at increased acid  
241 concentrations was attributed to incomplete dissociation of the weakly acidic functional  
242 groups within each resin [20]. Reduced  $Ni^{2+}$  and  $Co^{2+}$  recovery by Purolite S950+ and  
243 Amberlite IRC 748 (an alternative iminodiacetic-functionalized polystyrene-DVB resin) at  
244 lower pH has also been reported elsewhere [21, 22] and accredited to the competition for  
245 active adsorption sites between hydronium and metal ions in solution.

246 Interestingly, complete extraction of  $Fe^{3+}$  by S950+ was observed under all studied  
247 conditions, with only minor suppression of  $Al^{3+}$  beyond 0.3 M  $H^+$  (Figure 6). When compared  
248 to S930+ (Figure 8), it is evident that  $Fe^{3+}$  and  $Al^{3+}$  pose a greater barrier to trace metal  
249 removal for S950+, where selectivity towards  $Fe^{3+}$  and  $Al^{3+}$  would reduce the removal  
250 capacity for other metals present. In both cases, decreasing solution acidity would allow for  
251 more effective metal recovery from jarosite wastes.

252

253 The effect of increased sulfate concentration in the PLS was investigated for both weak acid  
254 exchange resins through addition of ammonium sulfate. With the exception of  $Fe^{3+}$  and  $Al^{3+}$ ,  
255 the uptake of all other metal ions by S950+ was suppressed as sulfate concentration  
256 increased. It is suggested that the formation of anionic metal complexes, incompatible with  
257 cation exchange mechanisms, is responsible for the reduced extraction. This theory also  
258 explains the quantitative extraction of  $Fe^{3+}$  and  $Al^{3+}$  (Figure 7), which do not form stable  
259 anionic sulfate complexes at the studied pH (1.40), and so remain accessible to cation

260 exchange by aminophosphonic functional groups. Beyond 2 M sulfate<sup>-</sup>, the extraction of Cu<sup>2+</sup>,  
261 Mn<sup>2+</sup>, and Zn<sup>2+</sup> begins to increase. Given that these metals are likely present as anionic  
262 complexes at this point, removal by true ion exchange is unlikely, suggesting an alternative  
263 removal process under these conditions. Further experimental work would be required to  
264 identify this mechanism.

265

266 Figure 9 displayed the results of increased PLS sulfate concentration on metal extraction  
267 by S930+, the behavior of which was substantially different than that of S950+. In this case,  
268 Cu<sup>2+</sup> and Fe<sup>3+</sup> were quantitatively removed at all sulfate concentrations, with Fe<sup>3+</sup> extraction  
269 becoming only slightly suppressed at 4 M SO<sub>4</sub><sup>2-</sup>. In contrast to figure 6, extractions of metals  
270 by S930+ tended to increase with increased sulfate, particularly Co<sup>2+</sup> and Zn<sup>2+</sup>. This trend is  
271 likely a result of increased solution ionic strength, through addition of sulfate, increasing the  
272 strength of chelate formations, as previously reported for iminodiacetic silica gels in  
273 chromatographic studies for a range of divalent transition metals [23]. The difference in  
274 behavior between the two weak acid resins under different sulfate concentrations could be  
275 used advantageously in an engineered process. By applying aminophosphonic functionalized  
276 resin where sulfate concentrations are low, and iminodiacetic resin where ionic strength may  
277 be a limiting factor, the recovery of metals could be maximized in a range of conditions.

278

### 279 **4.3 Strong acid functionalised resins**

280 As seen from Figures 10 and 12, both strong acid resins display little selectivity at higher pH,  
281 however S957 is shown to preferentially extract trivalent metal cations below pH 1 while all  
282 metal uptake on M31 is suppressed. Similar results were found in previous literature [24]  
283 where trivalent metal cations were found to be preferentially extracted at very high acidities by  
284 Diphonix<sup>TM</sup>, a dual-mechanism resin with sulfonic and gem-diphosphonic acid functionalities  
285 in nitric media, whereas the sulfonic acid resin Bio-Rad<sup>TM</sup> AG MP-50 displayed much lower

286 selectivity at these higher proton concentrations. Suppression of metal uptake at higher ionic  
287 strengths by M31 indicates a cation exchange mechanism for both divalent and trivalent  
288 metal cations with the sulfonic acid functionality (Figure 13). The same can be said for S957  
289 regarding the divalent metal cations, however the negligible effect of increased ionic strength  
290 on trivalent metal cation extraction suggests the phosphonic acid functionality has a chelating  
291 interaction with  $Al^{3+}$  and  $Fe^{3+}$ , but does not interact strongly with the  $M^{2+}$  ions in solution  
292 (Figure 11). The synthesis and use of bifunctional sulfonic-phosphonic acid functionality  
293 resins like S957 was introduced to improve both the selectivity and kinetics of metal ion  
294 extraction using strong acid resins [25]. The extraction kinetics are not explored in this study;  
295 however, the added selectivity is clearly shown. M31 has little potential with regard to  
296 selective valuable metal extraction from jarosite waste, but has potential for bulk ion removal.  
297 The lack of selectivity by S957 rules the resin out for specific metal removal, but there is  
298 potential for it to be used as a pretreatment to remove the less valuable iron from solution  
299 under very acidic conditions to maximize the performance of subsequent exchange columns  
300 (Figure 14).

301

302

## 303 **5 CONCLUSIONS**

304 Based on the results of the current work, the following conclusions are drawn:

- 305 - Weak base and strong base resins are not appropriate resin functionalities for the  
306 targeted recovery of metals from a jarosite leaching PLS. More work is needed to see  
307 if these resins are more applicable to an alkaline leaching process using ammonium  
308 hydroxide ( $NH_4OH$ ) or sodium cyanide ( $NaCN$ ) as a lixiviant.
- 309 - Strong acid resins are not appropriate for targeted metal recovery due to the  
310 suppression of uptake by high ionic strength. Purolite S957 with mixed phosphonic

311 and sulfonic acid functionality may be better utilized to remove  $\text{Fe}^{3+}$  from the PLS  
312 before passing it through the recovery stage.

313 - No single resin is capable of recovering all the value from the PLS stream while  
314 leaving the non-valuable iron behind. From the data presented in Figure 3 and 4, it is  
315 proposed that M4195 is appropriate for removing  $\text{Cu}^{2+}$ ,  $\text{Co}^{2+}$ ,  $\text{Ni}^{2+}$  and  $\text{Zn}^{2+}$  from the  
316 PLS, after which  $\text{Al}^{3+}$  and  $\text{Mn}^{2+}$  should pass through unaffected. After this initial  
317 recovery stage, due to the reduction in concentration of the other metals by previous  
318 columns, the  $\text{Mn}^{2+}$  and  $\text{Al}^{3+}$  can be recovered by the strong acid resin M31 to leave a  
319 barren solution. A schematic outline for a potential jarosite treatment process is given  
320 in Figure 14. A sand filter is used before the treatment column to remove particulate  
321 and colloidal material that may affect the performance of ion exchange columns.

322

323

324

325

326

327

## 328 **6 ACKNOWLEDGMENTS**

329 The authors would like to acknowledge the members of the Separations and Nuclear  
330 Chemical Engineering Research (SNUCER) group at the University of Sheffield who all  
331 assisted with this work in some capacity. Thank you to Prof. Neil Hyatt and Dr. Claire  
332 Corkhill in MIDAS, University of Sheffield for use of analytical equipment. Thank you to Dr  
333 Gabriella Kakonyi at the Kroto Research Institute at the University of Sheffield for ICP-MS  
334 analysis. Funding was provided by the Department of Chemical and Biological Engineering  
335 at the University of Sheffield, as part of their start-up scheme. This research did not receive  
336 any specific grant from funding agencies in the public, commercial, or not-for-profit sectors.

337 **7 REFERENCES**

- 338 [1] Pappu, A.; Saxena, M.; Asolekar, S.R. (2006) Hazardous jarosite use in developing non-  
339 hazardous product for engineering application. *J. Haz. Mat.*, 137: 1589.
- 340 [2] Pappu, A.; Saxena, M.; Asolekar, S.R. (2007) Solid wastes generation in India and their  
341 recycling potential in building materials. *Build. Environ.*, 42: 2311.
- 342 [3] Kerolli-Mustafa, M.; Curkovic, L.; Fajkovic, H.; Roncevic, S. (2015) Ecological Risk  
343 Assessment of Jarosite Waste Disposal. *Croat. Chem. Acta*, 88: 189.
- 344 [4] Underwood, B.E.; Kruse, N.A.; Bowman, J.R. (2014) Long-term chemical and biological  
345 improvement in an acid mine drainage-impacted watershed. *Environ. Monit. Assess.*,  
346 186: 7539.
- 347 [5] Johnson, D.B.; Hallberg, K.B. (2005) Acid mine drainage remediation options: a review.  
348 *Sci. Total Environ.*, 338: 3.
- 349 [6] Mukherjee, T.K. (2004) Processing of secondary resources for sustainable development  
350 in the metallurgical industries. IIM Presidential Address,  
351 [www.igcar.gov.in/transiim/2004/iim2004.pdf](http://www.igcar.gov.in/transiim/2004/iim2004.pdf) (retrieved 28/11/2016).
- 352 [7] Pappu, A.; Saxena, M.; Asolekar, S.R. (2006) Jarosite characteristics and its utilisation  
353 potentials. *Sci. Total Environ.* 359: 232.
- 354 [8] <https://www.lme.com/> (retrieved 28/11/2016)
- 355 [9] Hubicki, Z.; Kołodyńska, D. (2012) Selective Removal of Heavy Metal Ions from Waters  
356 and Waste Waters Using Ion Exchange Methods. *Ion Exchange Technologies*,  
357 DOI:10.5772/51040.
- 358 [10] Tanaka, S.; Harada, A.; Nishihama, S; Yoshizuka, K. (2012) Selective Recovery of  
359 Platinum Group Metals from Spent Automobile Catalyst by Integrated Ion Exchange  
360 Methods. *Separ. Sci. Technol.*, 47: 1369.

- 361 [11] Gomes, H.I.; Jones, A.; Rogerson, M.; Greenway, G.M.; Lisbona, D.F.; Burke, I.T.;  
362 Mayes. W.M. (2016) Removal and recovery of vanadium from alkaline steel slag  
363 leachates with anion exchange resins. *J. Environ. Manage.*, 187: 384.
- 364 [12] Gomes, H.I.; Jones, A.; Rogerson, M.; Burke, I.T.; Mayes. W.M. (2016) Vanadium  
365 removal and recovery from bauxite residue leachates by ion exchange. *Environ. Sci.*  
366 *Pollut. Res.*, 23: 23034.
- 367 [13] Kuz'min, V.I.; Kuz'min, D.V. (2014) Sorption of nickel and copper from leach pulps of  
368 low-grade sulfide ores using Purolite S930 chelating resin. *Hydrometallurgy*, 141: 76.
- 369 [14] Bukowska, A.; Bukowski, W.; Pytel, M. (2015) Scavenging properties of the  
370 polyamine functionalized gels based on the glycidyl methacrylate terpolymers. *Open*  
371 *Journal of Polymer Chemistry*, 5: 63. <http://dx.doi.org/10.4236/ojchem.2015.54008>
- 372 [15] Green, B.R.; Hancock, R.D. (1982) Useful resins for the selective extraction of  
373 copper, nickel and cobalt. *J. South Afr. Inst. Min. Metall.* Oct: 303.
- 374 [16] Diniz, C.V.; Ciminelli, V.S.T.; Doyle, F.M. (2005) The use of chelating resin Dowex M-  
375 4195 in the adsorption of selected heavy metal ions from manganese solutions.  
376 *Hydrometallurgy*, 78: 147.
- 377 [17] Diniz, C.V.; Doyle, F.M.; Ciminelli, V.S.T. (2002) Effect of pH on the absorption of  
378 selected heavy metal ions from concentrated chloride solutions by the chelating resin  
379 dowex M4195. *Sep. Sci. Technol.* 37: 3169.
- 380 [18] Wolowicz, A.; Hubicki, Z. (2012) The use of chelating resin of a new generation  
381 Lewatit Monplus TP220 with bis-picolylamine functional groups in the removal of  
382 selected metal ions from acidic solutions. *Chem. Eng. J.* 197: 493.
- 383 [19] Casas, J.M.; Crisostomo, G.; Cifuentes, L. (2005) Speciation of the Fe(II)–Fe(III)–  
384 H<sub>2</sub>SO<sub>4</sub>–H<sub>2</sub>O system at 25 and 50 °C. *Hydrometallurgy*, 80: 254.
- 385 [20] Outola, P.; Leinonen, V.; Ridell, M.; Lehto, J. (2001) Acid/Base and Metal Uptake  
386 Properties of Chelating and Weak Base Resins. *Solvent Extr. Ion Exc.*, 19: 743.

- 387 [21] Deepatana, A.; Valix, M.; (2006) Recovery of nickel and cobalt from organic acid  
388 complexes: Adsorption mechanisms of metal-organic complexes onto  
389 aminophosphonate chelating resin. *J. Haz. Mat.*, 137: 925.
- 390 [22] Zainol, Z.; Nicol, M.J. (2009) Ion exchange equilibria of Ni<sup>2+</sup>, Co<sup>2+</sup>, Mn<sup>2+</sup> and Mg<sup>2+</sup>  
391 with iminodiacetic acid chelating resin Amberlite IRC 748. *Hydrometallurgy*, 99: 175.
- 392 [23] Bashir, W.; Paull, B. (2002) Ionic strength, pH and temperature effects upon  
393 selectivity for transition and heavy metal ions when using chelation ion chromatography  
394 with an iminodiacetic acid bonded silica gel column and simple inorganic eluents. *J.*  
395 *Chromatogr. A.*, 942: 73.
- 396 [24] Chiarizia, R.; Horwitz, E. P.; Gatrone, R. C.; Alexandratos, S. D.; Trochimczuk, A. Q.;  
397 Crick, D. W. (1993) Uptake of metal ions by a new chelating ion-exchange resin. Part 2:  
398 Acid dependencies of transition and post-transition metal ions, *Solvent Extr. Ion Exc.*, 11:  
399 967.
- 400 [25] Alexandratos, S.D.; Natesan, S. (1999) Ion-selective polymer-supported reagents:  
401 the principle of bifunctionality, *European Polymer Journal*, 35: 431.
- 402

403 Table 1. Elemental composition of industrial jarosite and potential resource recovery value

404 [1-3, 6-8]

Element symbol	Composition		Recovery value	
	% max.	% min	£ max	£ min
Fe	31.43	23.66	£20,978	£15,791
Cu	0.1043	0.97	£6,448,945	£693,428
Al	3.613	0.752	£7,219,635	£1,502,675
Co	0.0038	0.00304	£128,001	£102,401
Ni	0.0093	0.197	£121,696	£113,844
Mn	0.639	8.243	£1,269,570	£391,401
Zn	10.9	0.197	£34,426,013	£26,034,277
<b>Total</b>			<b>£49,634,837</b>	<b>£28,853,817</b>

405

406

407

408

409

410

411

412

413

414

415

416

417 Table 2. Ion exchange resins tested for metal extraction from simulated jarosite leach  
 418 solutions (N/A = data not available from supplier, PA = polyacrylic, PS = polystyrene, DVB =  
 419 divinylbenzene; capacity converted to eq/L from manufacturer specification sheets).

Name	Acronym	Functionality	Capacity (eq/L)	Polymer Matrix	Moisture Content (%)	Particle Size (µm)
Purolite S985	S985	Polyamine	2.3	PA-DVB	52-57	300-1200
Dowex M4195	M4195	Bis-picolylamine	1.1 - 1.3	PS-DVB	40-60	297-841
Purolite S910	S910	Amidoxime	1.3	PA-DVB	52-60	300-1200
Purolite S930Plus	S930+	Iminodiacetic acid	1.6	PS-DVB	52-60	425-1000
Purolite S950Plus	S950+	Aminophosphonic acid	1.3	PS-DVB	60-68	N/A
Purolite S957	S957	Phosphonic/sulfonic	0.64	PS-DVB	55-70	N/A
Dowex M31 SA	M31	Sulfonic acid	4.7	PS-DVB	50-54	420-1190

420

421

422

423

424 Table 3. pH<sub>50</sub> values for the extraction of tested metal ions as a function of pH on M4195,  
 425 calculated from extraction curves (<sup>a</sup>NC = not calculated, <sup>b</sup>predicted using linear regression of  
 426 4 data points.)

Element	pH <sub>50</sub>	Element	pH <sub>50</sub>
Al <sup>3+</sup>	NC <sup>a</sup>	Ni <sup>2+</sup>	0.54
Co <sup>2+</sup>	1.35	Mn <sup>2+</sup>	NC <sup>a</sup>
Cu <sup>2+</sup>	-0.51 <sup>b</sup>	Zn <sup>2+</sup>	1.35
Fe <sup>3+</sup>	1.75		

427 <sup>a</sup>NC = not calculated, <sup>b</sup>predicted using linear regression of 4 data points

428

429 Table 4.  $pH_{50}$  values for the extraction of tested metal ions as a function of pH on S950+ and

430

S930+, calculated from extraction curves.

S950+				S930+			
Element	$pH_{50}$	Element	$pH_{50}$	Element	$pH_{50}$	Element	$pH_{50}$
Al <sup>3+</sup>	NC <sup>a</sup>	Ni <sup>2+</sup>	1.92	Al <sup>3+</sup>	3.06 <sup>b</sup>	Ni <sup>2+</sup>	1.53
Co <sup>2+</sup>	1.51	Mn <sup>2+</sup>	1	Co <sup>2+</sup>	2.08 <sup>b</sup>	Mn <sup>2+</sup>	3.72 <sup>b</sup>
Cu <sup>2+</sup>	1.26	Zn <sup>2+</sup>	1.31	Cu <sup>2+</sup>	0.51	Zn <sup>2+</sup>	NC <sup>a</sup>
Fe <sup>3+</sup>	NC <sup>a</sup>			Fe <sup>3+</sup>	0.72		

431

<sup>a</sup>NC = not calculated, <sup>b</sup>predicted using linear regression of 4 data points

432

433

434 Table 5.  $pH_{50}$  values for the extraction of tested metal ions as a function of pH on S957 and

435

M31, calculated from extraction curves.

S957				M31			
Element	$pH_{50}$	Element	$pH_{50}$	Element	$pH_{50}$	Element	$pH_{50}$
Al <sup>3+</sup>	0.05	Ni <sup>2+</sup>	0.68	Al <sup>3+</sup>	-0.08	Ni <sup>2+</sup>	0.18
Co <sup>2+</sup>	0.66	Mn <sup>2+</sup>	0.64	Co <sup>2+</sup>	0.12	Mn <sup>2+</sup>	0.02
Cu <sup>2+</sup>	0.64	Zn <sup>2+</sup>	0.66	Cu <sup>2+</sup>	0.10	Zn <sup>2+</sup>	0.21
Fe <sup>3+</sup>	NC <sup>a</sup>			Fe <sup>3+</sup>	0.05		

436

<sup>a</sup>NC = not calculated

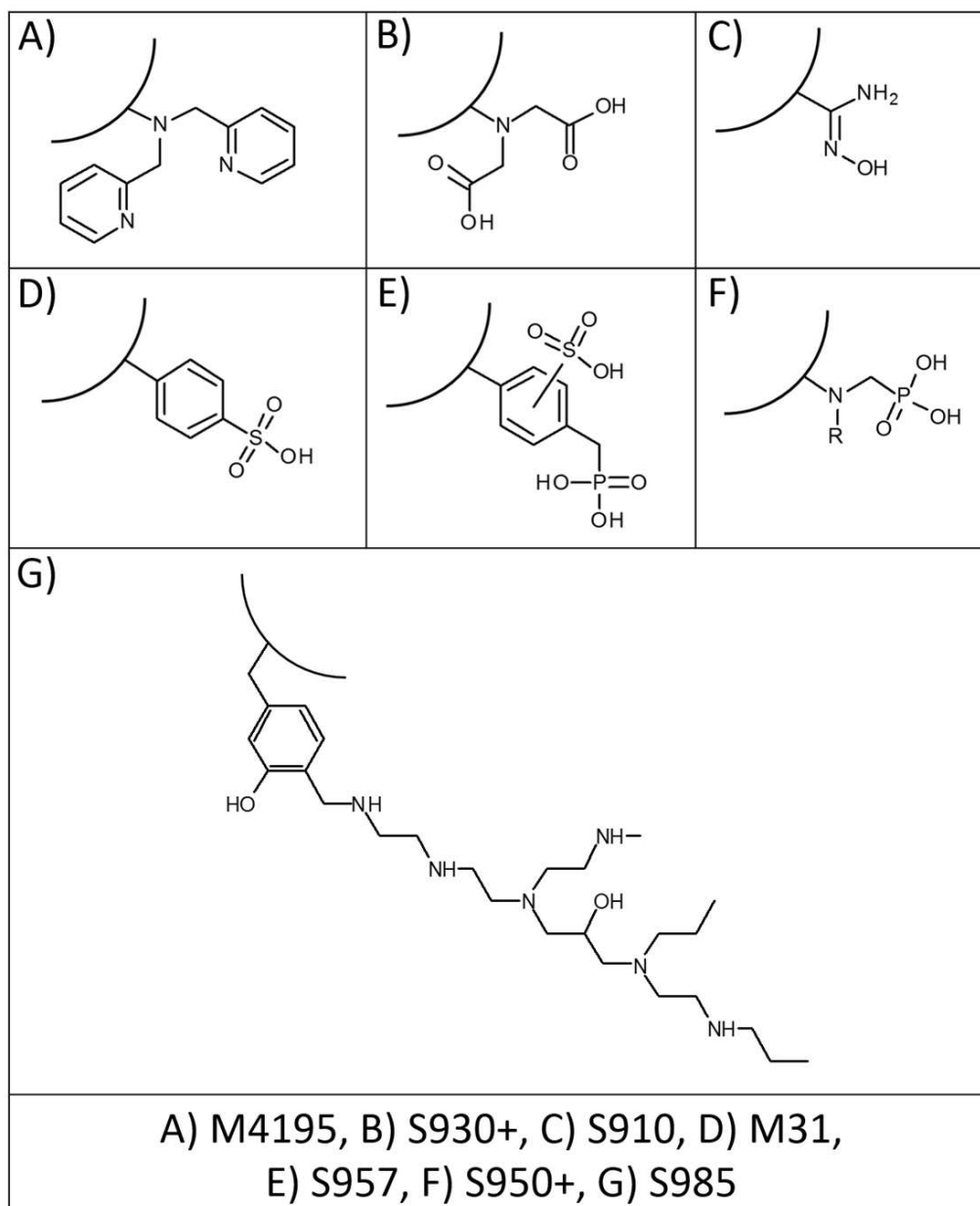
437

438

439

440 Fig. 1. Chemical structure of ion exchange resin functionalities (curved line = bulk resin

441 matrix, e.g. PS-DVB).



442

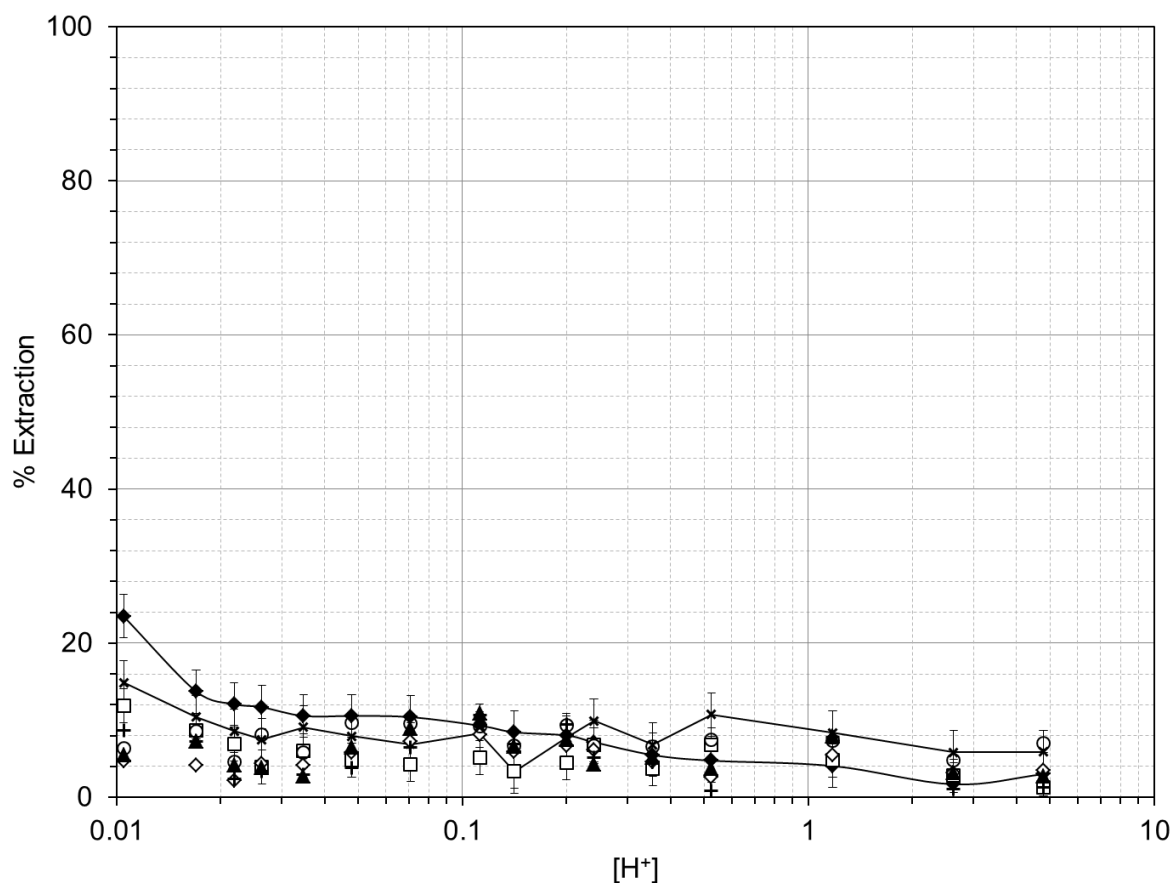
443

444

445

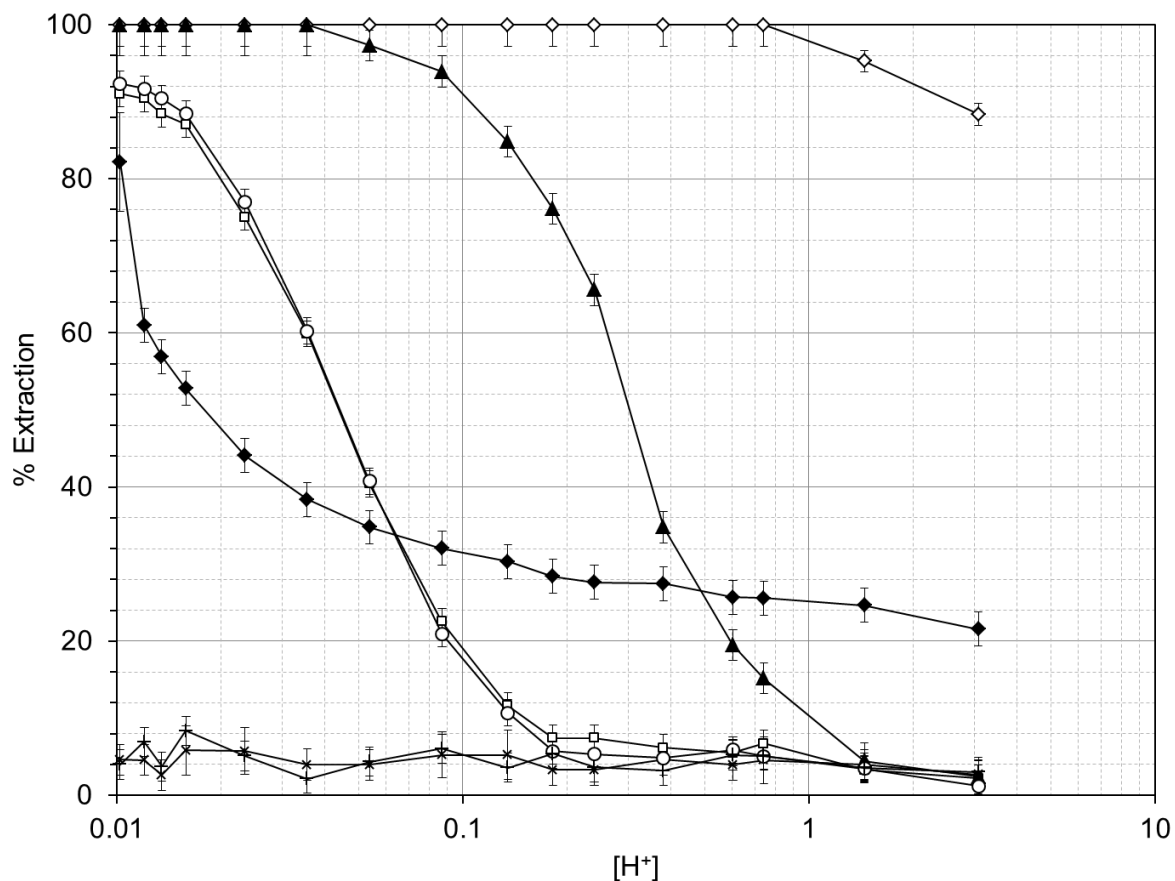
446

447 Fig. 2. Extraction of metal ions as a function of sulfuric acid concentration on S985. Al(III) =  
448 +, Co(II) = □, Cu(II) = ◇, Fe(III) = ◆, Ni(II) = ▲, Mn(II) = ×, Zn(II) = ○  
449



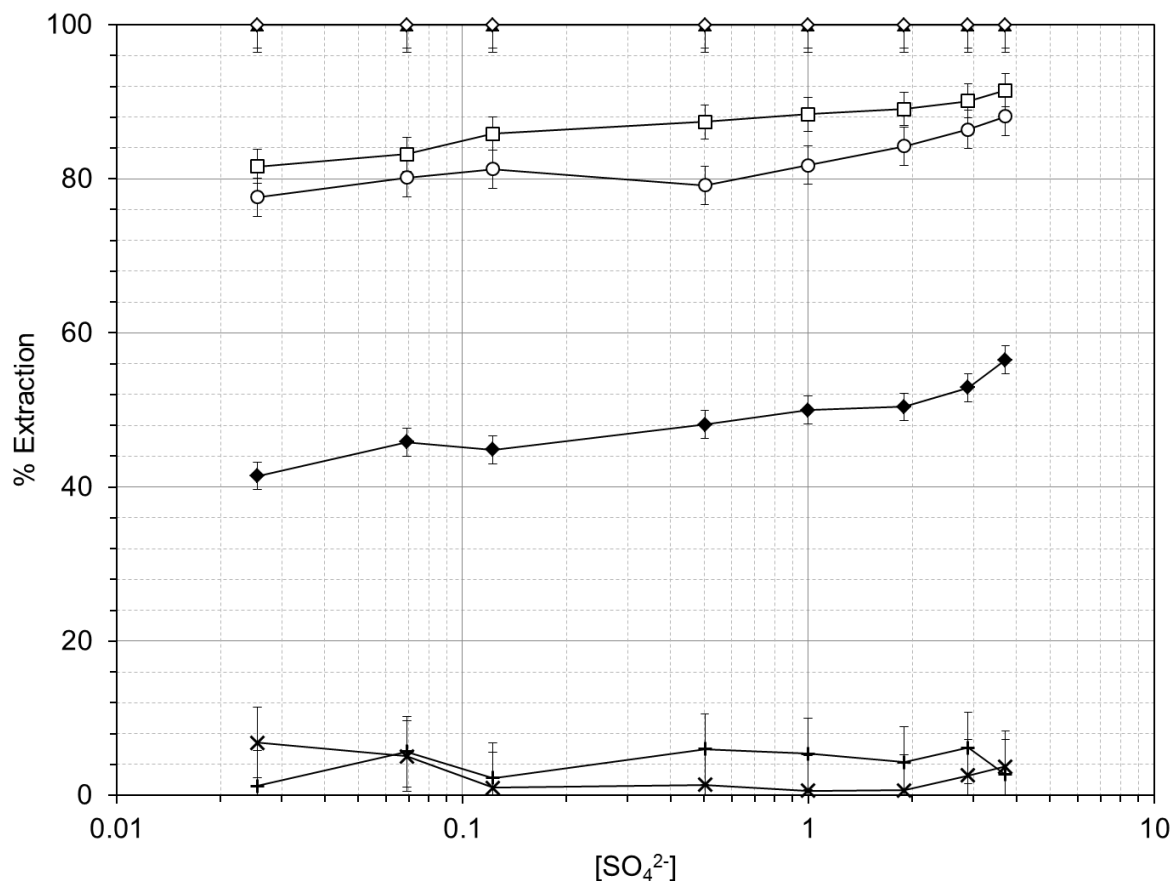
450  
451  
452  
453  
454  
455  
456  
457  
458  
459

460 Fig. 3. Extraction of metal ions as a function of sulfuric acid concentration on M4195. Al(III) =  
461 +, Co(II) = □, Cu(II) = ◇, Fe(III) = ◆, Ni(II) = ▲, Mn(II) = ×, Zn(II) = ○  
462



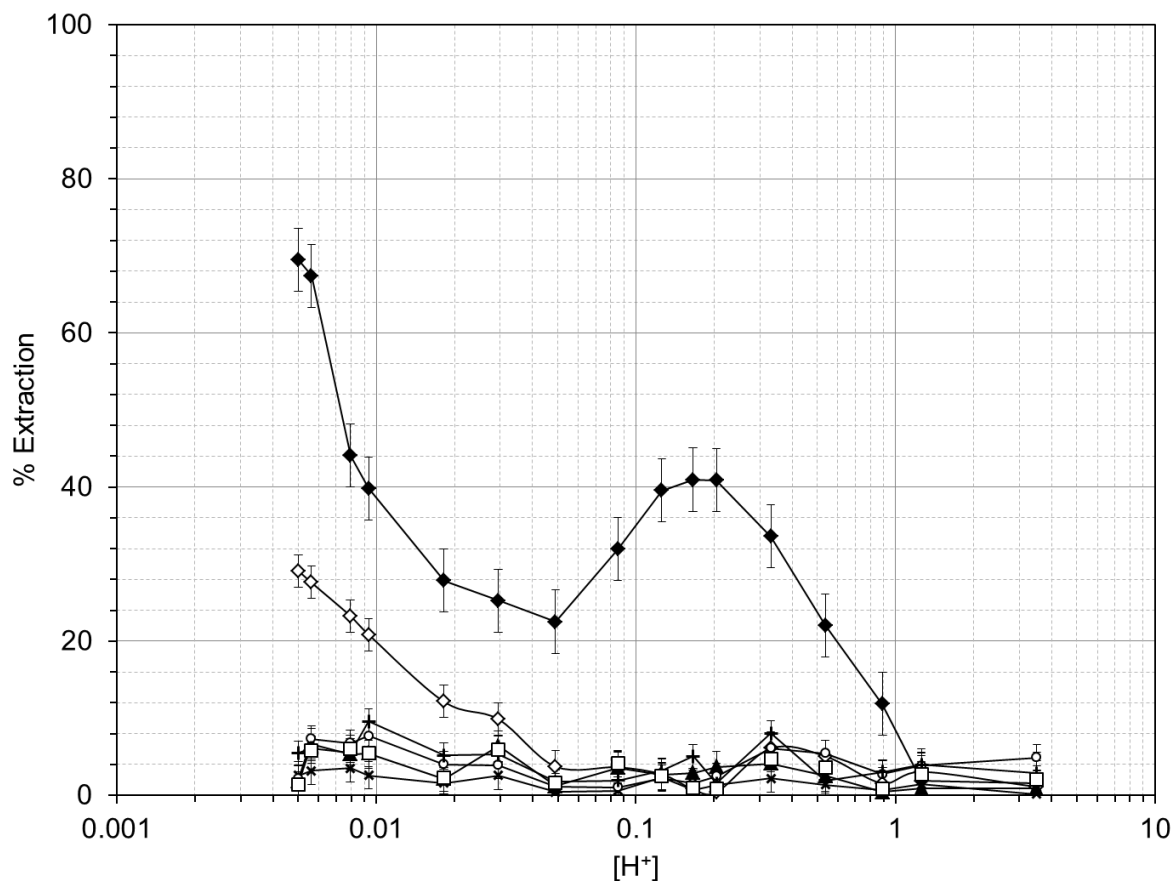
463  
464  
465  
466  
467  
468  
469  
470  
471  
472

473 Fig. 4. Extraction of metal ions as a function of ammonium sulfate concentration on M4195  
474 at pH 1.55. Al(III) = +, Co(II) = □, Cu(II) = ◇, Fe(III) = ◆, Ni(II) = ▲, Mn(II)= ×, Zn(II) = ○  
475



476  
477  
478  
479  
480  
481  
482  
483  
484  
485

486 Fig. 5. Extraction of metal ions as a function of sulfuric acid concentration on S910. Al(III) =  
487 +, Co(II) = □, Cu(II) = ◇, Fe(III) = ◆, Ni(II) = ▲, Mn(II) = ×, Zn(II) = ○  
488

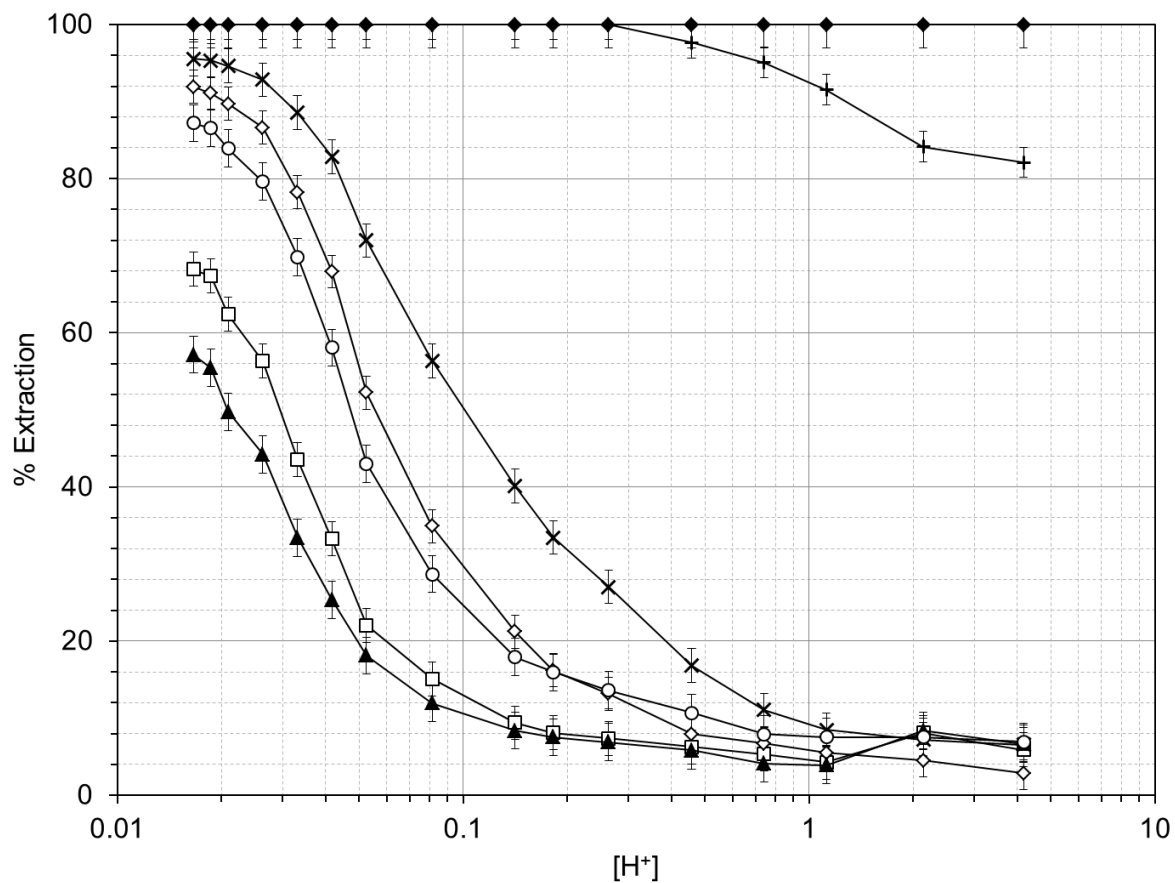


489  
490  
491  
492  
493  
494  
495  
496  
497  
498

499 Fig. 6. Extraction of metal ions as a function of sulfuric acid concentration on S950+. Al(III) =

500 +, Co(II) = □, Cu(II) = ◇, Fe(III) = ◆, Ni(II) = ▲, Mn(II) = ×, Zn(II) = ○

501



502

503

504

505

506

507

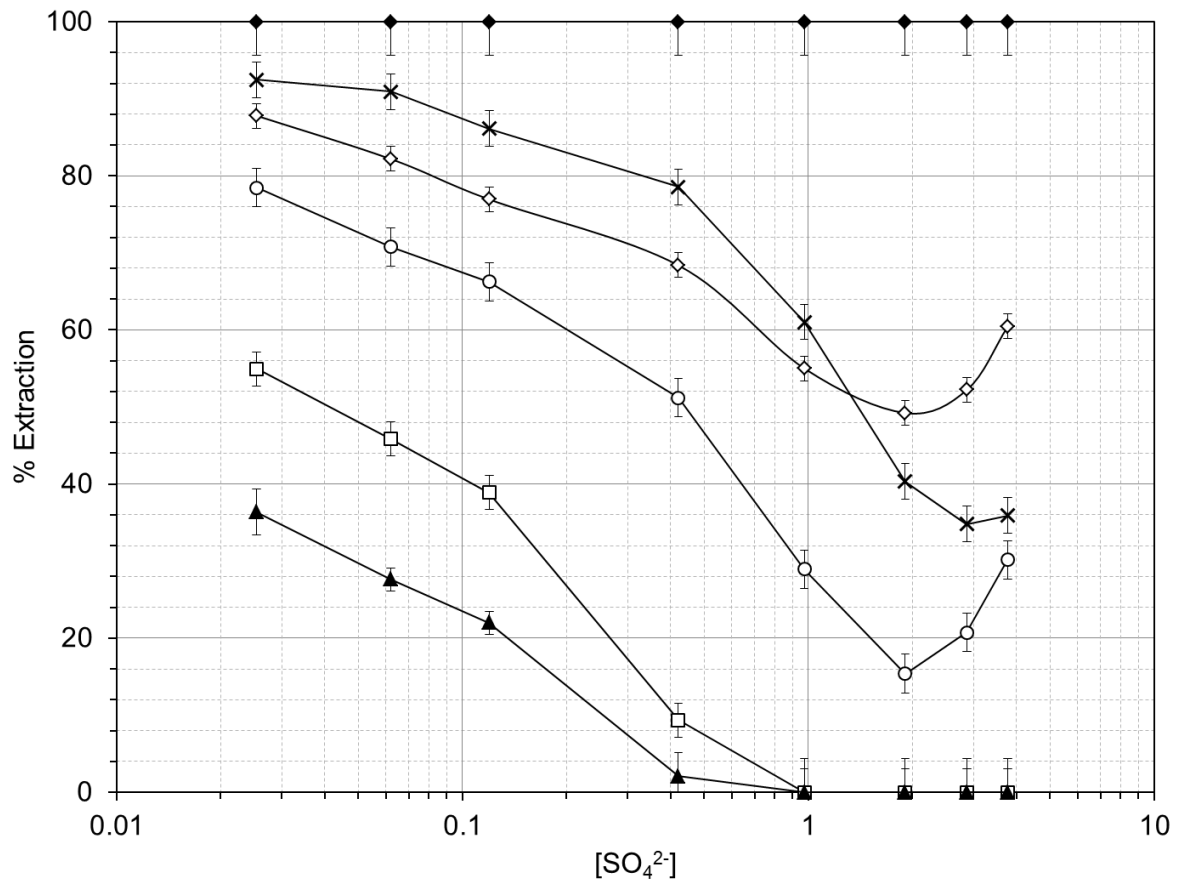
508

509

510

511

512 Fig. 7. Extraction of metal ions as a function of ammonium sulfate concentration on S950+ at  
513 pH1.40 Al(III) = +, Co(II) = □, Cu(II) = ◇, Fe(III) = ◆, Ni(II) = ▲, Mn(II)= ×, Zn(II) = ○  
514

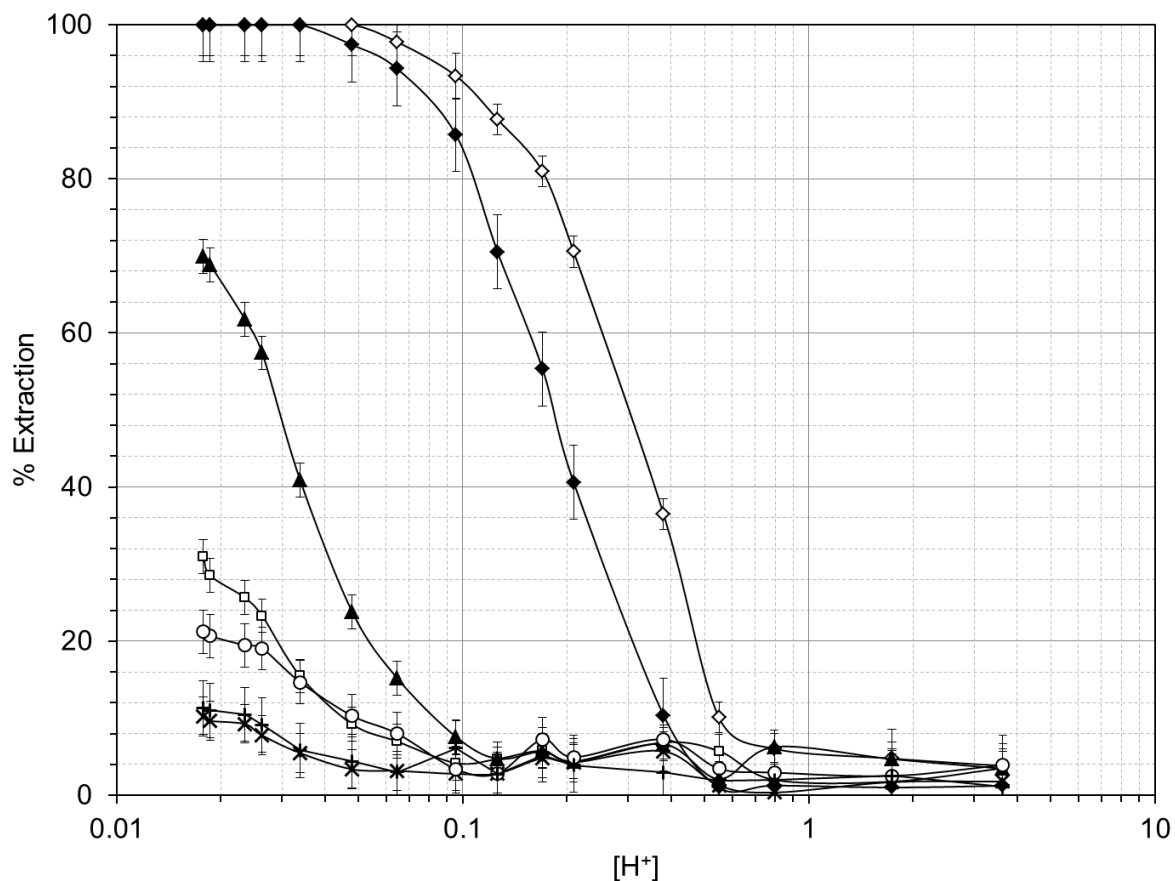


515  
516  
517  
518  
519  
520  
521  
522  
523  
524

525 Fig. 8. Extraction of metal ions as a function of sulfuric acid concentration on S930+. Al(III) =

526 +, Co(II) = □, Cu(II) = ◇, Fe(III) = ◆, Ni(II) = ▲, Mn(II)= ×, Zn(II) = ○

527



528

529

530

531

532

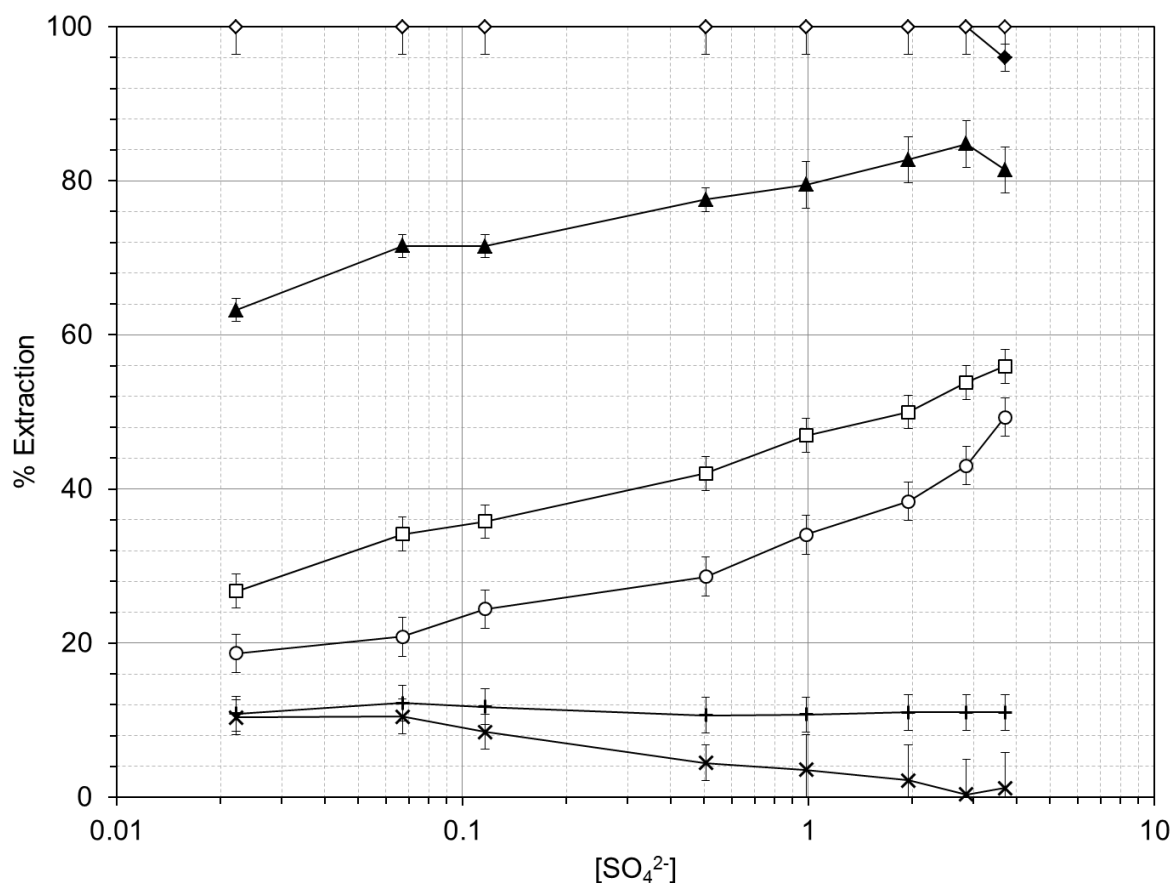
533

534

535

536

537 Fig. 9. Extraction of metal ions as a function of ammonium sulfate concentration on S930+ at  
538 pH1.45 Al(III) = +, Co(II) = □, Cu(II) = ◇, Fe(III) = ◆, Ni(II) = ▲, Mn(II)= ×, Zn(II) = ○  
539

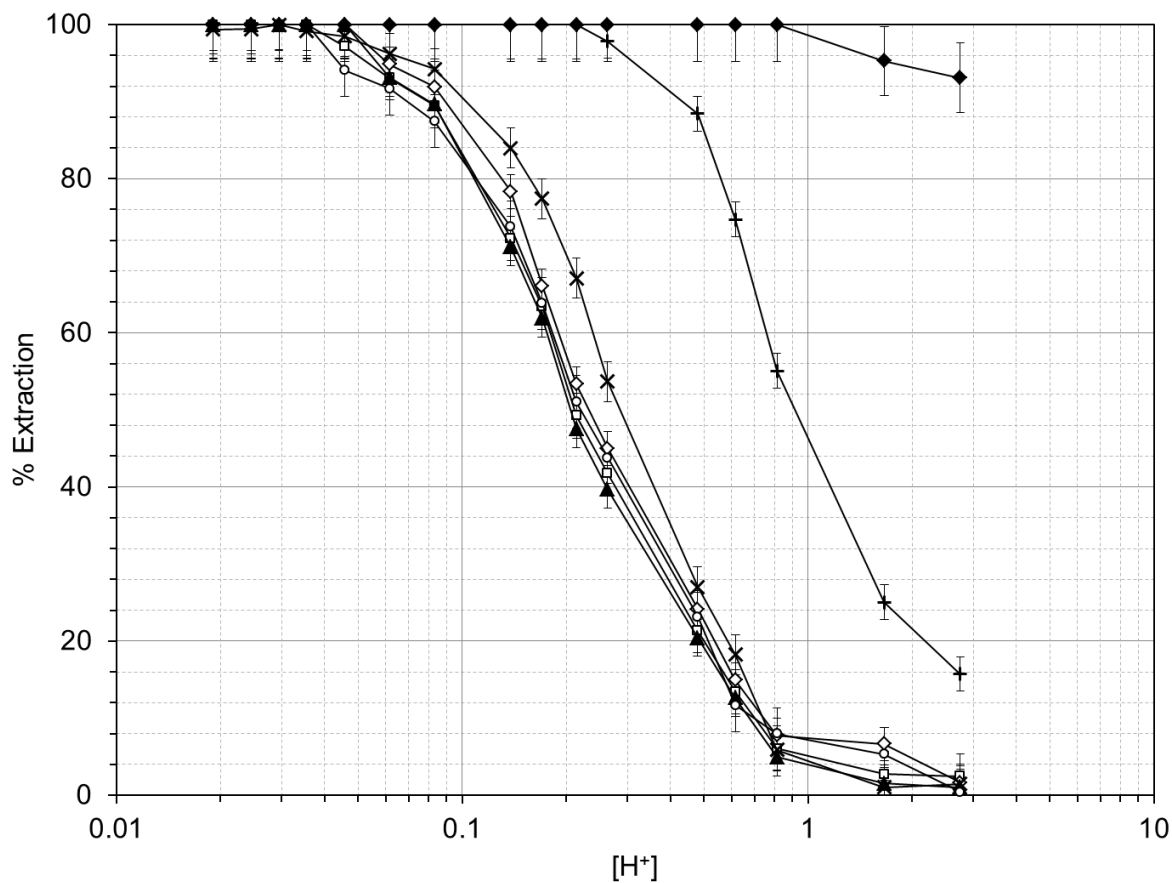


540  
541  
542  
543  
544  
545  
546  
547  
548  
549

550 Fig. 10. Extraction of metal ions as a function of sulfuric acid concentration on S957. Al(III) =

551 +, Co(II) = □, Cu(II) = ◇, Fe(III) = ◆, Ni(II) = ▲, Mn(II) = ×, Zn(II) = ○

552



553

554

555

556

557

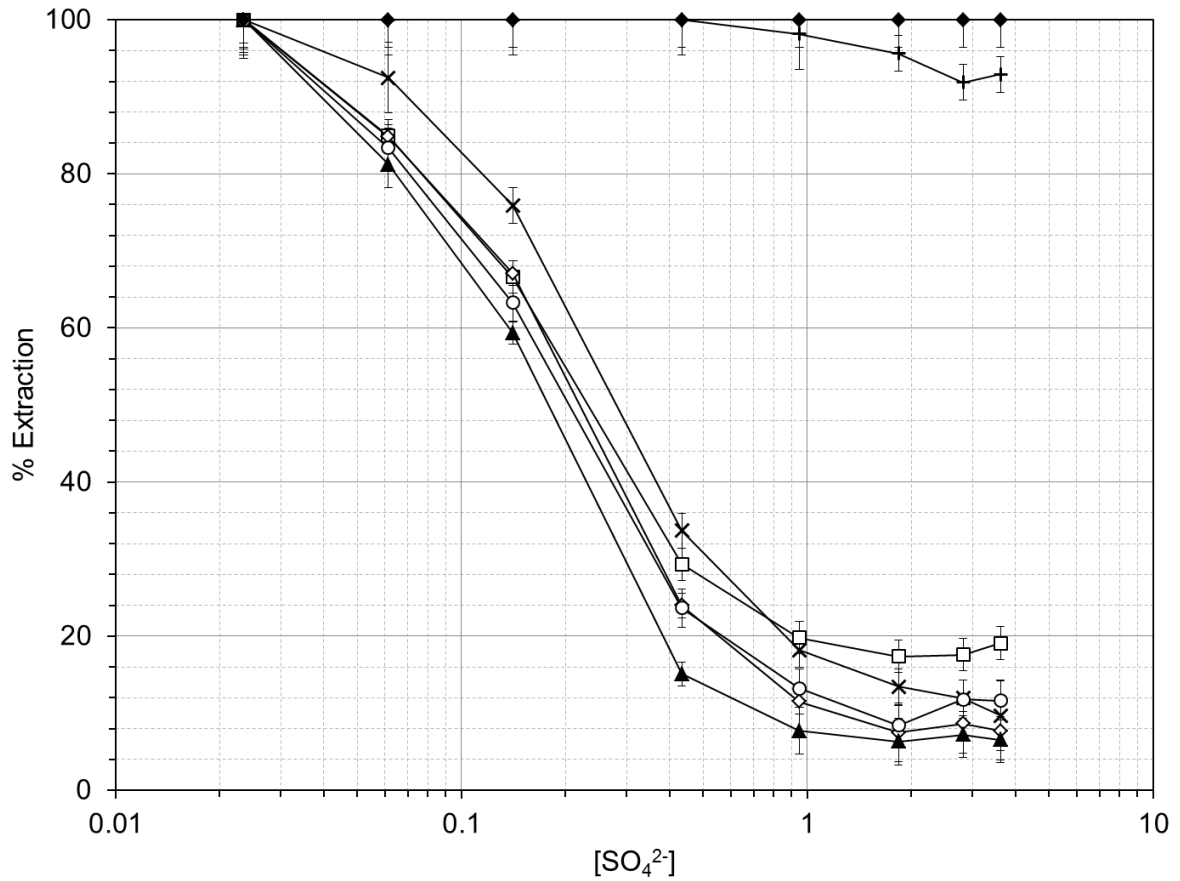
558

559

560

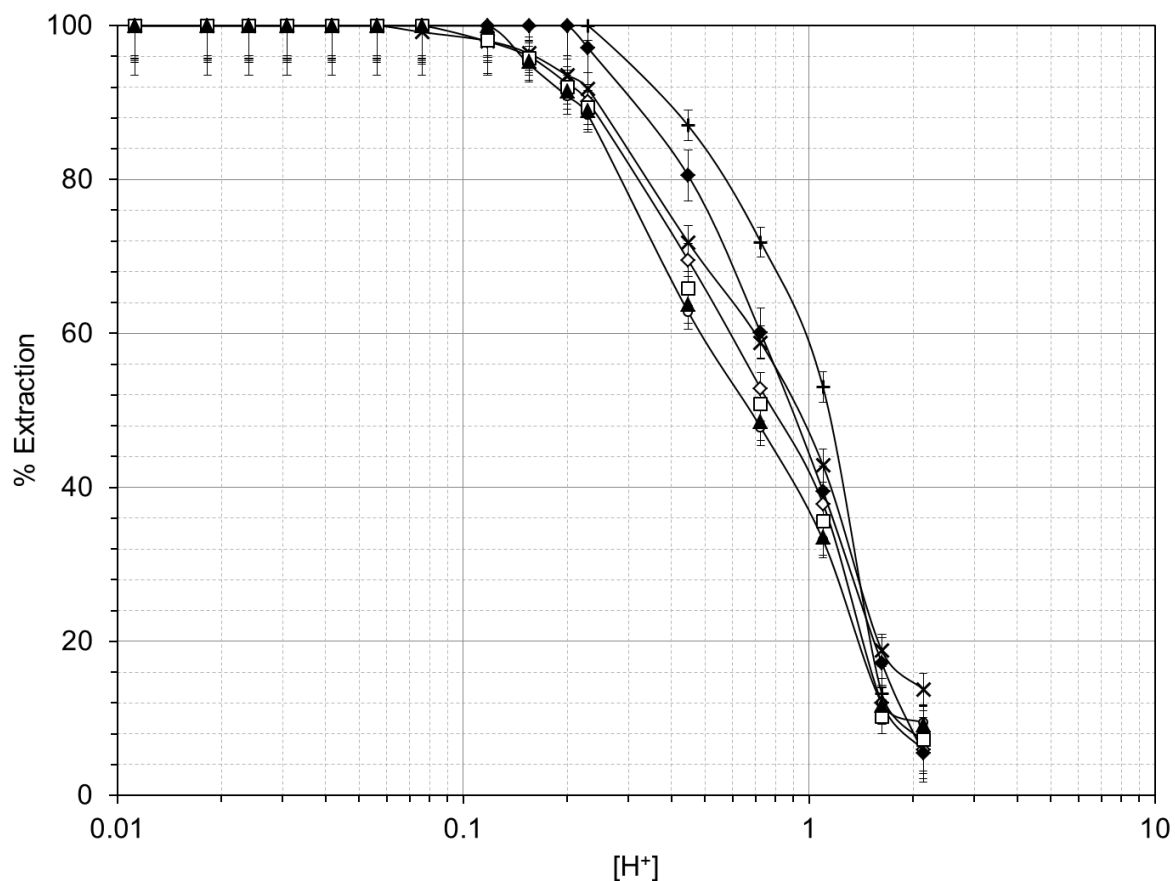
561

562 Fig. 11. Extraction of metal ions as a function of ammonium sulfate concentration, pH 1.35,  
563 on S957. Al(III) = +, Co(II) = □, Cu(II) = ◇, Fe(III) = ◆, Ni(II) = ▲, Mn(II)= ×, Zn(II) = ○  
564



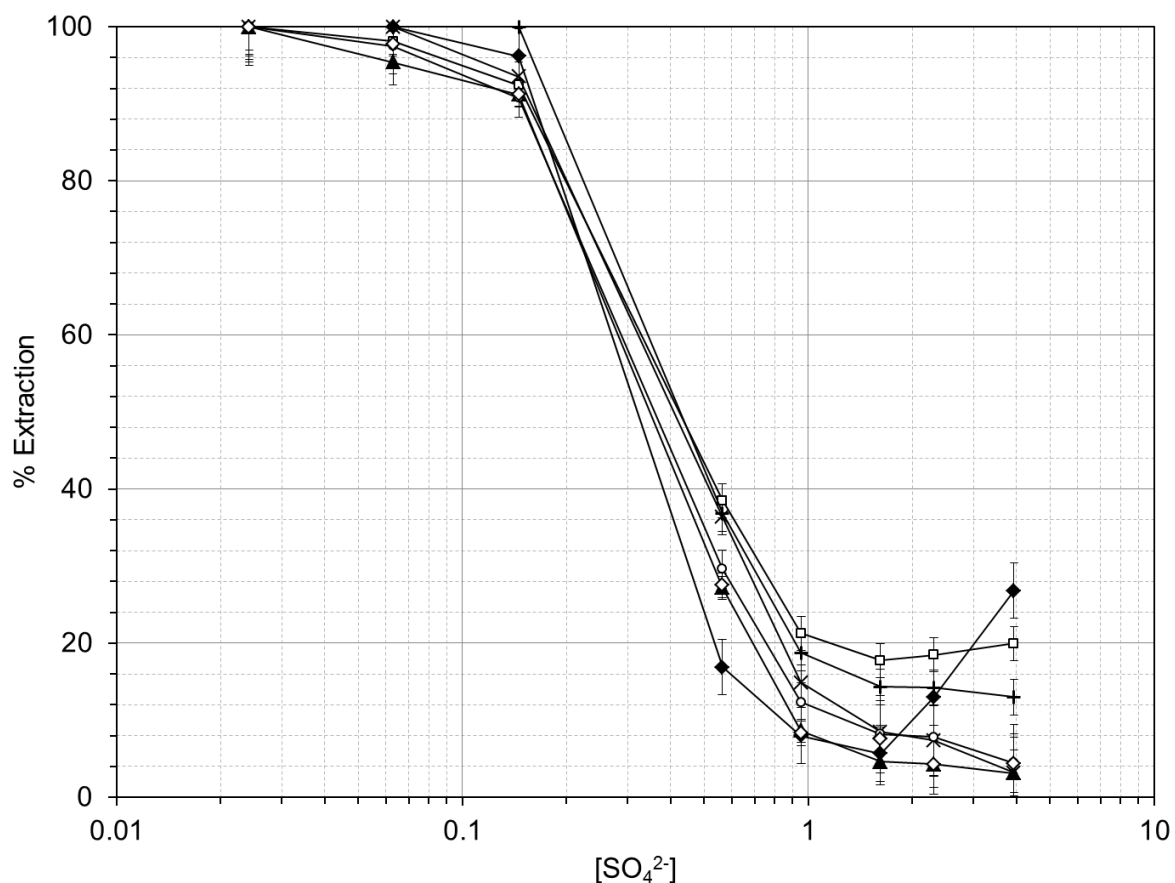
565  
566  
567  
568  
569  
570  
571  
572  
573

574 Fig. 12. Extraction of metal ions as a function of sulfuric acid concentration on M31. Al(III) =  
575 +, Co(II) = □, Cu(II) = ◇, Fe(III) = ◆, Ni(II) = ▲, Mn(II) = ×, Zn(II) = ○  
576



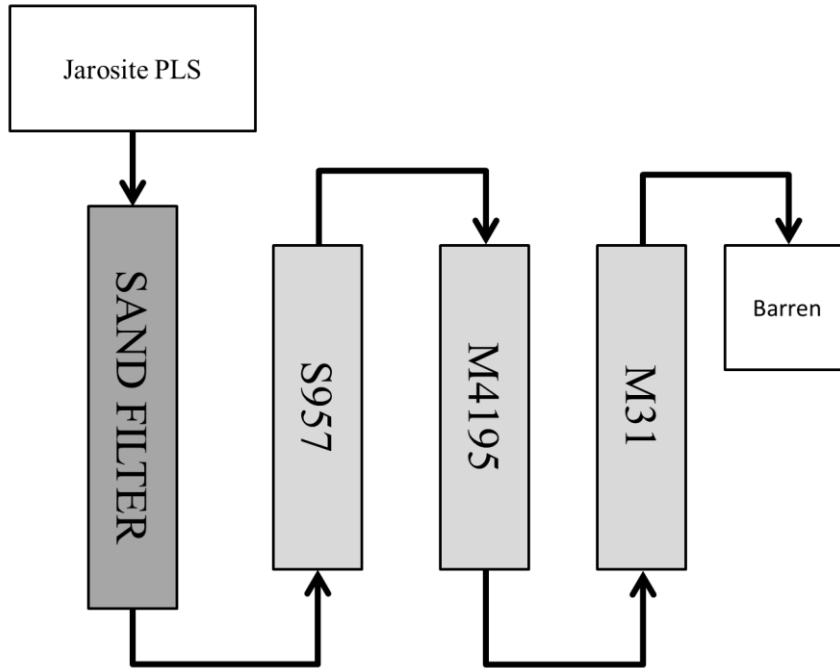
577  
578  
579  
580  
581  
582  
583  
584  
585  
586

587 Fig. 13. Extraction of metal ions as a function of ammonium sulfate concentration, pH 1.45,  
588 on M31. Al(III) = +, Co(II) = □, Cu(II) = ◇, Fe(III) = ◆, Ni(II) = ▲, Mn(II) = ×, Zn(II) = ○  
589



590  
591  
592  
593  
594  
595  
596  
597  
598  
599

600 Fig. 14. Schematic ion exchange recovery process for the treatment of acidic sulfate media  
601 containing  $\text{Cu}^{2+}$ ,  $\text{Fe}^{3+}$ ,  $\text{Ni}^{2+}$ ,  $\text{Co}^{2+}$ ,  $\text{Zn}^{2+}$ ,  $\text{Mn}^{2+}$ , and  $\text{Al}^{3+}$ , as expected following jarosite leaching.  
602



603